Rotational spectra and temperature evaluation of C_2 molecules produced by pulsed laser irradiation to a graphite–water interface

Kotaro Saito, Tetsuo Sakka,[a] and Yukio H. Ogata
Institute of Advanced Energy, Kyoto University, Uji, Kyoto 611-0011, Japan

(Received 21 April 2003; accepted 6 August 2003)

Temperature of an ablation plume produced by pulsed laser irradiation to a graphite target submerged in water was evaluated as a function of time by analyzing the emission spectra of C_2 molecules. The method is based on the determination of rotational temperature from the rotational spectra of the (0,0) Swan band of C_2 molecules. In the time range shorter than 1000 ns from the ablation laser pulse, the rotational temperature of ~6000 K was obtained. After 1000 ns it decreases rapidly, in contrast to the temperature obtained for the irradiation in air, where the decrease of the temperature is rather slow. The linewidth obtained as one of the fitting parameters suggests the high density and high pressure of this region. Temporal behavior of the laser ablation plume in water is discussed. © *2003 American Institute of Physics.* [DOI: 10.1063/1.1614431]

I. INTRODUCTION

Irradiation of a pulsed laser to a solid target can result in an explosive emission of atoms, ions, and electrons from the target surface. This pulsed laser ablation has attracted intensive attention, because it can be used in various applications. Many researchers have investigated the laser ablation in vacuum or in dilute gases, aiming at the clarification of gas phase chemical reactions,[1–4] thin film fabrications,[5–7] cluster formations,[8,9] and also, solid surface modifications.[10,11]

On the other hand, laser ablation of a solid target immersed in liquid shows a behavior different from that in vacuum or in a dilute gas environment.[12–17] The ablated species are highly confined to a small region in the vicinity of the solid–liquid interface due to the inertia of liquid.[18,19] It is expected that this region has an instantaneous high density of energetic species, high pressure, and high temperature. Actually, it has been reported that small crystallites of diamond are formed by the irradiation of a solid target immersed in water[20] or in organic liquids.[21,22] The formation of the ''metastable'' phase should be explained by the pressure–temperature phase diagram, as well as the kinetics of the cluster formation. It may be possible that the final size of the crystallites can be controlled by the growth time. Therefore, in order to understand the cluster formation reaction, *the temperature and pressure as a function of time must be experimentally evaluated*.

In spite of the vast richness observed by the irradiation of a solid target immersed in liquid, techniques diagnosing the plumes in liquid are very limited, since techniques based on vacuum systems, such as mass spectroscopy, are not applicable when liquid is present. However, optical spectroscopy seems to be a possible solution for our purpose, i.e., the information of the plume region can be obtained at a detector placed outside the cell by emitted light. Analyses of spectral profiles and line intensities are expected to provide information inside the plume.[23]

In the present article, we evaluate the rotational temperature of C_2 molecules in the plume region. The method is based on the fitting of the observed rovibronic spectra known as the Swan band[24] to a theoretical calculation. A few nm width of the spectral range within the Swan band of the (0, 0) transition was used for the fitting. The rotational temperature was obtained as an adjustable parameter. By analyzing the spectra at various delay times from the excitation pulse, the temperature was evaluated as a function of time. Furthermore, we obtained some information on the collision frequency in the plume region from the linewidth obtained as another adjustable parameter.

The temperature evaluation using the Swan system of C_2 molecules has been applied to various objects, such as the laser ablation plume in vacuum or in gaseous atmosphere,[25–27] an acoustic cavitation produced by an ultrasonic irradiation of liquids,[28] and astronomic objects.[29,30] However, for *the ablation plume produced on a solid target immersed in liquids*, very limited data of temperature are available so far.[15,31] Furthermore, it is not known whether the plume region is in a gaseous state with the molecules rotating rather freely or if it is in a condensed state where molecular rotation is considerably hindered. In the previous article, we estimated plasma electron temperature by fitting the continuous spectral component of the emission spectra to Planck's formula of blackbody radiation.[15] Also, the vibrational temperature of C_2 molecules in the ablation plume surrounded with water was estimated by the Boltzmann plot based on the band head intensities of the $\Delta\nu=-1$ bands of the Swan system.[31] However, both of them have a weakness in their accuracy and reliability, i.e., the former used the continuous spectra to which considerable contribution from the broadened line spectra is present, whereas the latter used the band head intensities to which the contribution from adjacent vibrational bands cannot be completely removed, and also, the intensity saturation by the self-absorption effect

[a]Author to whom correspondence should be addressed; electronic mail: t-sakka@iae.kyoto-u.ac.jp

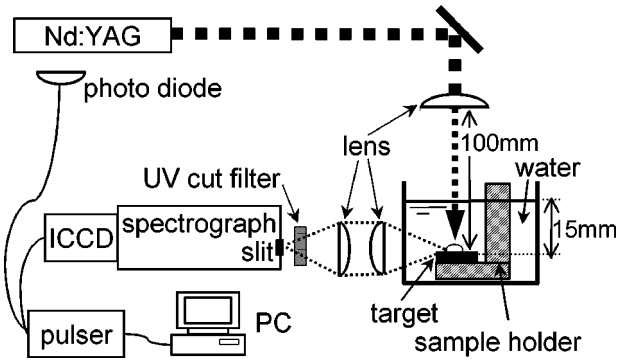

FIG. 1. Schematic diagram of the experimental setup.

could not be corrected properly. This work shows that the rotation of C_2 molecules is quite a good thermometer for the plume region produced by the laser irradiation to a solid target submerged in liquid. The method in the present study would give a rather *reliable rotational temperature* even for poorly resolved rotational spectra, because the fitting to the theoretical spectra is performed for the spectral profile in a certain range of the spectral band. According to the temperature data and other information, the characteristics of the plume region produced at a solid–liquid interface and its time evolution will be thoroughly discussed.

II. EXPERIMENT

A schematic diagram of our experimental setup is given in Fig. 1. The graphite target was a polycrystalline isotropic block ($d=1.77$ g/cm^3), the purity of which was 99.99%. The target was mounted on a target holder made of Teflon and placed in a UV/visible-grade quartz cell filled with water. Doubly distilled water purchased from Nacalai Tesque was used as received. The thickness of the water covering the sample was 15 mm.

A Q-switched Nd:YAG laser with a wavelength of 1064 nm and pulse duration of about 20 ns was focused by a lens with 100 mm focal length onto a target. The irradiation beam was normal to the surface of the water and also to the graphite target. The energy of the pulse was about 70 mJ. The laser spot size at the focus was ~ 0.087 mm, which was evaluated by the 2σ diam of the Gaussian beam profile obtained by scanning a 5 μm slit with measuring the transmitted light by a Joule meter. Then, the fluence at the focal point is calculated to be about 1.2 kJ/cm^2, if the influence of the reflection and the refraction at the liquid surface and the energy absorption in the light path through the water were negligible. This irradiation condition does not cause a breakdown without the target.

The emission spectra were obtained by using double-dispersion spectrograph ($f=1$ m, Ritsu Oyo Kogaku, MC100N) equipped with two 1800 grooves/mm diffraction gratings. The lateral emission from the plume was collected and guided into the spectrograph. The entrance slit width was set to 20 μm. An intensified charge-coupled device (ICCD) (Princeton Instruments, ICCD-1024MTDGE/1) was used as a detector. The measurement was performed in the spectral range from 512 to 518 nm, where the $\Delta\nu=0$ bands of the Swan system of C_2 molecules were observed. The instrumental function was obtained by using the 632.8 nm line of a He–Ne laser, and was very well approximated by the Lorentzian profile with the full width at half maximum (FWHM) of 0.03 nm. The spectral resolution of this system is limited by the correlation between the adjacent pixels of the ICCD detector. The ICCD exposure was performed by applying a high-voltage gate pulse generated by a gate pulser (Princeton Instruments, PG-200) to the intensifier. The trigger for the high-voltage pulse was obtained by detecting a leak pulse from the laser oscillator using a fast photodiode. The rising edge of the trigger pulse was used as a delay time origin. The duration of the gate pulse was set to 100 ns. The time delay from the ablation laser pulse was varied within the range from 50 to 2000 ns. In order to improve the signal-to-noise ratio, averaging of the spectra obtained for five successive ablation pulses was performed.

III. THEORETICAL SPECTRA

We calculated the spectra from the theoretical intensity and the location of each rotational line with taking account of the spectral broadening. In general, the Boltzmann plot method is a rather simple procedure to obtain the rotational temperature. However, in this method it is necessary to identify a sufficient number of well-isolated rotational lines, which should not overlap one another. In the case of rotational lines of the C_2 Swan band, both the upper and lower states have triplet splitting, which causes complicated overlapping of the neighboring lines. Furthermore, the results in the present work showed that each line is considerably broadened in comparison with the well-separated lines observed in vacuum or in dilute gas atmosphere. Therefore, we compared the theoretical spectra in a wide spectral range with experiments in order to achieve the highest accuracy in the determination of the rotational temperature.

The Swan band of the C_2 molecules originates in the electronic transition from the $d\,^3\Pi_{g,v'}$ state to the $a\,^3\Pi_{u,v''}$ state. In the calculation of the spectra, we need the frequency, intensity, and width of each rotational line. The spectral terms of diatomic molecules are given in the literature.[24] The emission coefficient $\varepsilon_{J'i',J''i''}$ of a particular rotational line in a band (v',v'') is given as follows:

$$\varepsilon_{J'i',J''i''}=CS_{J'i',J''i''}\sigma_{ul}^4\exp\left(\frac{-F_{v'i'}(J')}{k_BT_{\mathrm{rot}}}\right), \tag{1}$$

where $S_{J'i',J''i''}$, $F_{v'i'}(J')$, σ_{ul} are the rotational intensity factor (Hönl–London factor),[24] the rotational energy of the upper level, and the wavenumber of the spectral line, respectively, and T_{rot} and k_B are the rotational temperature and the Boltzmann constant, respectively. The subscripts J and i denote the rotational quantum number and the multiplicity, respectively. The Frank–Condon factor is included in the constant C, since the calculation is performed within the same vibrational transition. This expression is used when the rotational states are in thermal equilibrium. Kovacs[32,33] has given the formulas of rotational intensity factors $S_{J'i',J''i''}$ for various types of transitions and Hund's couplings, including the $^3\Pi-{}^3\Pi$ transition. In the calculation of $F_{v'i'}(J')$ and σ_{ul},

the molecular constants given by Pellerin *et al.*[25] were used. The theoretical spectra were obtained by the summation of all the major rotational lines, each of which has an integrated intensity of $\varepsilon_{J'i',J''i''}$ with a common broadening profile. This spectrum was fit to an experimental spectrum by adjusting three parameters, namely, the rotational temperature, linewidth, and scaling factor.

As mentioned above, the broadening function of the rotational lines should be assumed in the calculation. Other than the broadening mechanism discussed later, an instrumental broadening in our spectroscopic measurement is not negligible. The instrumental function obtained from the measured He–Ne laser spectrum by our system agreed with the Lorentzian profile.

There seems to be three possible intrinsic broadening mechanisms in the present system, namely, the Doppler, Stark, and collision broadening. The first one gives the Gaussian profile, while the others give the Lorentzian profile. The full width at half maximum of the Doppler-broadened line is described as

$$\Delta\omega_{\mathrm{DW}} = 2(\ln 2)^{1/2}(\omega_0/c)(2k_BT/M_A)^{1/2}, \tag{2}$$

where ω_0, c, T, and M_A are the resonance angular frequency, light velocity, absolute temperature, and mass number, respectively. By substituting the parameters into Eq. (2), with assuming the temperature of 5000 K, which corresponds to the typical plasma temperature obtained for the laser ablation plume in dilute gases,[27] Doppler broadening of 5.3×10^{-3} nm was obtained. This is an order of magnitude smaller than the instrumental width, suggesting that the convolution of the Gaussian distribution due to Doppler broadening gives only a weak effect on the line profile. Therefore, we employed the Lorentzian function to describe the line broadening in our analysis, because the convolution of the Lorentzian functions gives the Lorentzian.

The spectral range from 513.4 to 516.0 nm was used for the fitting, because the intensity of the band head seemed to be suppressed for some reasons. This misfit at the band head will be discussed later in Sec. V. Fitting to the theoretical spectra was performed using a computer program based on an iterative method to minimize the deviation from the experimental spectra. Rotational temperature and linewidth were determined as the parameters giving the best-fit spectrum.

IV. RESULTS

In Fig. 2, typical spectra obtained for the graphite target in water are shown as well as a spectrum obtained in air. Each plot is an accumulation of the spectra from five successive ablation events. The time delay from the laser irradiation is given in Fig. 2. It is obvious from the spectra that the clarity of the line feature is poor in the case of laser ablation in water compared with that in air, i.e., each rotational line overlapped considerably with the neighboring lines, especially when the delay time is short. However, we can still distinguish the rotational progression in the spectra obtained in water. Some spectra were observed as a superposition of the continuous spectral emission, which is mainly attributed

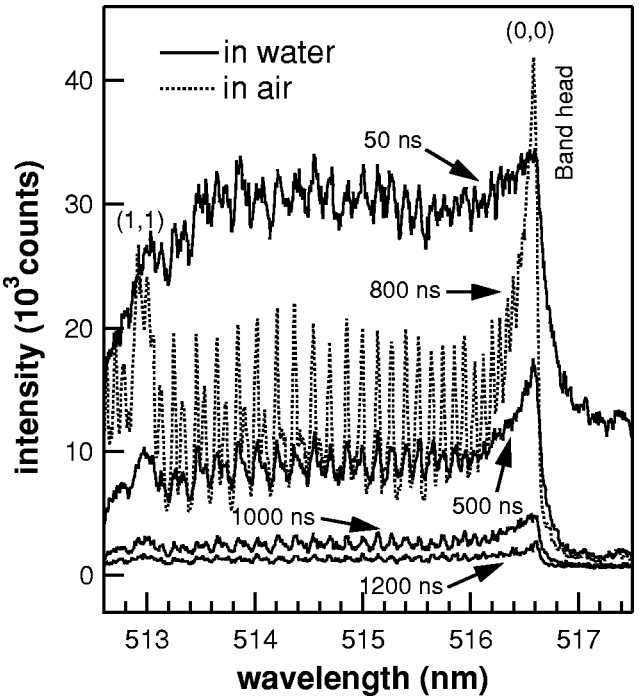

FIG. 2. Series of emission spectra obtained by irradiation of a pulsed Nd:YAG laser to graphite in water. The duration of the gate was set to be 100 ns. The time delay from the laser irradiation is given in the figure. The broken line is the spectrum obtained in air under similar experimental conditions.

to the plasma free electrons, and the Swan bands of C_2 molecules. The continuous part dominated the whole emission spectrum up to about 100 ns of the delay time. The contribution of the continuous spectrum is apparently observed in the wavelength range longer than 516.6 nm, i.e., longer than the band head of the (0,0) transition. While, later in the delay time, the continuous emission was greatly reduced and the series of line emissions became dominant in the spectra. After 2000 ns from the laser pulse, the emission intensity was reduced to the level lower than the detection limit.

In Fig. 3, the best-fit spectra are shown together with the observed spectra. They are representative spectra obtained at the delay time of 500 and 1000 ns. The spectrum obtained in water shows a considerably low band-head intensity compared with the corresponding theoretical spectrum obtained as a result of the fitting in the range from 513.4 to 516.0 nm. This strong suppression of the band head relative to the band tail occurs when the emission intensity is very high. On the other hand, shifts of the line peak position were not observed in the spectra in the entire time range during the measurement.

By adjusting the fitting parameters, a good fit of the spectral line profile to the theoretical spectra was obtained except for the vicinity of the band head. For comparison, we also measured the spectra for a target in air. The results in air show better agreement with the theoretical spectra, especially near the band head. The rotational temperature and the linewidth (FWHM) obtained as optimized fitting parameters are listed in Table I. These two adjusting parameters are plotted as a function of the delay time in Figs. 4 and 5, respectively. The rotational temperature was ~6000 K at 150 ns and de-

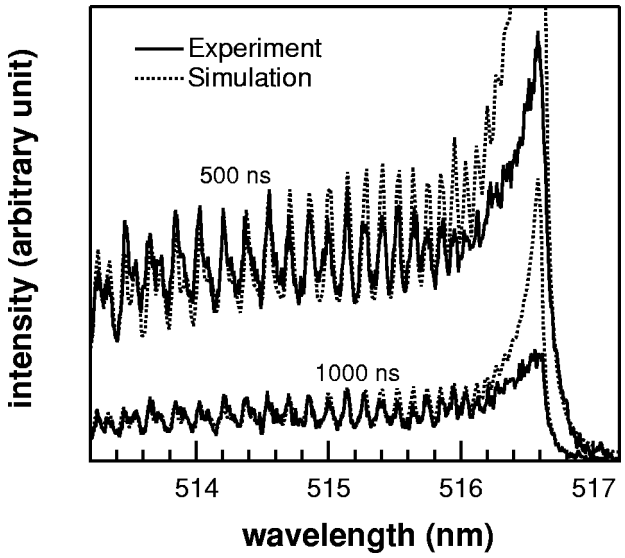

FIG. 3. Examples of experimental spectra and the optimized theoretical simulation of the (0,0) Swan system of C_2. The delay times were 500 and 1000 ns, and the gate width was 100 ns. Each spectrum is an accumulation of five spectra. The best-fit parameters obtained in the calculation are listed in Table I.

creased gradually. The intensity of the emitting light becomes very low for longer delay time due to the deactivation of C_2 molecules. However, the temperature was still very high at this stage. The linewidth obtained in the case of the target immersed in water was much larger than the instrumental width, in contrast to that in air where the linewidth is comparable to the instrumental width.

V. DISCUSSION

A. Spectra and analysis

The results in Fig. 2 show fairly resolved rotational lines, with line peak positions identical to those obtained in the gas phase. This indicates that C_2 molecules produced by the pulsed laser irradiation of a graphite target in water are rotating, and that the interaction of C_2 molecules with surrounded species is not as strong as the case of being dissolved in liquid. It is suggested from the shock wave measurement,[19] and also from the imaging of the light emitting region,[34] that the pressure can be as high as 1 GPa and the carbon atomic density as high as 10^{21} cm^{-3}. Nevertheless, the present results show that we can still consider this region, to which the ablation plume with intensive emission is confined, as a ''gas cavity,'' where C_2 molecules are rotating pretty freely.

TABLE I. Parameters obtained from the simulation of the C_2 Swan band.

	Delay time (ns)	Rotational temperature (K)	Linewidth (nm)
In liquid	150	5800±800	0.095±0.02
	500	5600±450	0.084±0.009
	1000	4500±200	0.062±0.004
	1200	3500±250	0.048±0.003
In air	500	5100±400	0.040±0.002
	800	5100±300	0.037±0.002
	1200	5300±350	0.034±0.002
	1500	4900±300	0.033±0.001
	2000	4300±200	0.032±0.002

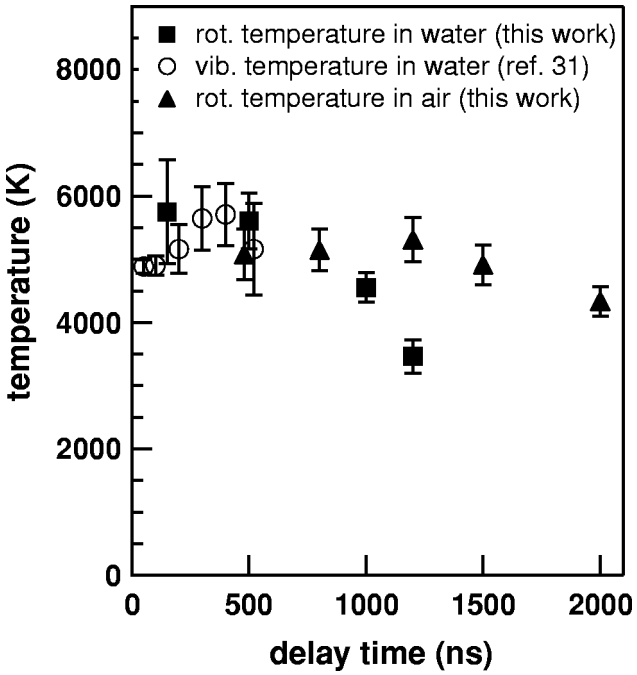

FIG. 4. Rotational temperature as a function of the delay time. Vibrational temperature obtained in previous work (see Ref. 31) by the Boltzmann plot using the series of vibrational bands in the $\Delta\nu=-1$ branch is also given in the figure.

When the theoretical spectrum is compared with the observation, the suppression of the emission intensity due to the self-absorption effect should be taken into consideration. In general, self-absorption is effective in an optically thick

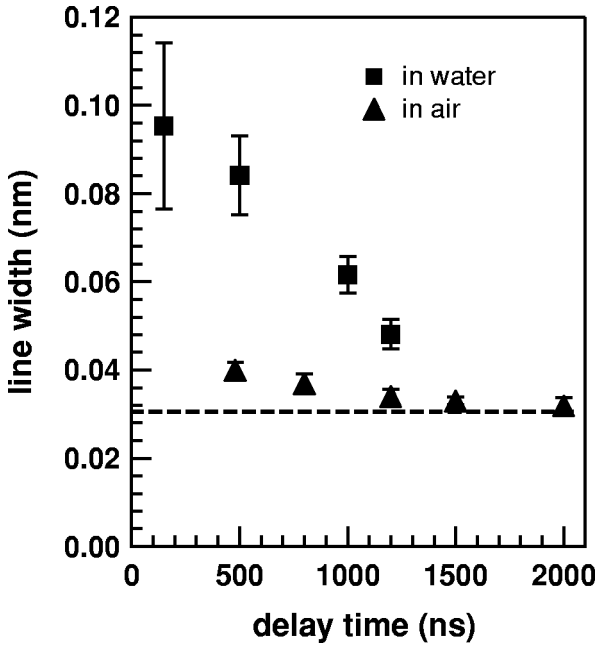

FIG. 5. Linewidth (FWHM) obtained as an optimized fitting parameter against the delay time. Broken line indicates the instrumental width.

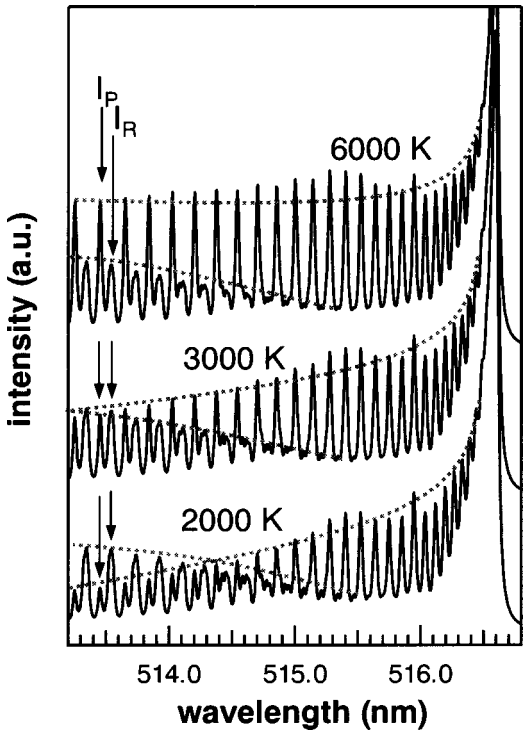

FIG. 6. Theoretical simulation of rotational bands at various temperatures. The linewidth was fixed to be 0.03 nm. Envelopes of the P and R branches are plotted by broken lines.

medium and for high radiation intensity or intensive transitions. If we assume the homogeneous plume with the thickness being L, the observed intensity I should be $(\varepsilon/\kappa)(1-e^{-\kappa L})$, where ε and κ are the emission and absorption coefficients, respectively.[35] The theoretical calculation of the spectra in the present work corresponds to the low-κ limit, where I tends to be εL. Hence, the suppression of the spectral intensity is $(1/\kappa L)(1-e^{-\kappa L})$. This quantity is sensitive to κL. If we assume κL to be 0.7 at the band tail and 3.5 at the band head, the suppression of the spectral intensity due to the self-absorption effect, which is pronounced mainly near the band head, can be quantitatively explained. Furthermore, we can show that the use of the band tail region gives rather accurate results for the temperature. It is known that the comparison of the two branches of the rotational lines (P and R) could be used for an estimation of the rotational temperature. Figure 6 shows the theoretical spectra at various temperatures. For example, we consider the intensity of two peaks observed apparently in the wavelength range from 513.4 to 513.6 nm, namely, one composed of $P_1(46)$, $P_2(45)$, and $P_3(44)$ ($\lambda = 513.451$, 513.448, and 513.460 nm, respectively), and the other composed of $R_1(17)$, $R_2(16)$, and $R_3(15)$ ($\lambda = 513.522$, 513.541, and 513.555 nm, respectively). If the instrumental width and the broadenings are sufficiently narrow, these two lines are well separated and the intensity ratio I_P/I_R can be quite accurately determined. As shown in Fig. 6, this ratio is sensitive to the temperature.[25] Also, Fig. 6 shows that the envelopes of the P and R branches are sensitive to the temperature, suggesting that fitting the theoretical spectra to experiments in the band-tail region is sufficient to obtain a quite reliable rotational temperature. Because the decrease in the intensity due to the self-absorption effect in this region, if any, is expected to be approximately the same for both branches, it is a reasonable solution to use the spectral range from 513.4 to 516.0 nm for the fitting procedure.

B. Rotational temperature

In Fig. 4, the time dependence of the rotational temperature obtained as an adjustable parameter is shown. Also in Fig. 4, the vibrational temperatures obtained previously by the Boltzmann plot using the band-head intensities of the Swan bands of $\Delta\nu = -1$ are shown.[31] Because the Boltzmann plot of the band-head intensity requires a pretty high intensity of the vibrational bands, the time range in which the temperature can be determined was limited up to ~ 500 ns. Also, the self-absorption effect at the band-head region may cause an error in this method. In the present study the fitting of the wide spectral range in the band-tail region enabled the determination of the rotational temperature for the delay time up to 1200 ns in water. The temperature in the case of a water-confined plume starts decreasing at ~ 1000 ns, while in air it decreased slower. Cooling of the plume by thermal diffusion in the time range of the present experiments is calculated to be negligible by using the thermal conductivity coefficient of water.[36] One possibility to explain the decrease in the temperature is the cooling due to radiation. Actually, at the delay time earlier than 50 ns, a very intense continuous spectrum was observed for the laser ablation in liquids. However, the prominent temperature decrease for the water-confined plume observed at the delay time of ~ 1000 ns appears exceedingly late compared with the time range of the intense emission. The decrease in temperature may be explained rather by the adiabatic expansion of the plume. For nonreversible adiabatic expansion, the temperature decrease is proportional to the volume increase with the proportionality coefficient of P_{ex}/C_v, where P_{ex} and C_v are the ambient pressure and the heat capacity at constant volume, respectively. By assuming that 10^{-8} g of water is expanding into the volume of 10^{-9} m^3 and also that C_v is less than that of liquid water, namely, 4.2 J K^{-1} g^{-1}, we obtain the temperature decrease of more than 2000 degrees. This rough estimation suggests that the expansion of the plume should be accompanied by a large temperature decrease.

C. Linewidth

The linewidth obtained as a best-fit parameter also gives some information about the plume. Figure 5 shows the linewidth (FWHM) as a function of the delay time. The broken line indicates the instrumental width determined by the measurement of the 632.8 nm line of the He–Ne laser. It is obvious that each rotational line was broadened in water much more than the instrumental width, while in air the width was almost identical to the instrumental width. The line broadening in water seems to be due to the collision broadening and/or the Stark broadening, as mentioned above. The frequency of collisions among atoms, ions, molecules, and free electrons in the water-confined plume must be much higher than in air.

According to our results, the Stark shift was not observed for the C_2 Swan bands as shown in Fig. 2. This does not mean the absence of the plasma free electrons, because the intense continuous spectral emission observed in the time range earlier than 50 ns is most probably caused by the bremsstrahlung or/and radiative recombination processes,[15] suggesting that the plasma electron density is very high. Also, the Stark shift of an Al atomic line is observed in the similar ablation plume produced at the aluminum–water interface.[35] The reason why we do not observe the Stark shift of the Swan band is probably merely due to a very small Stark shift coefficient for the Swan bands. On the other hand, the broadening of each line is clearly observed in the spectra. Since we are not aware of the Stark shift and broadening coefficients of C_2 molecules, it is not easy to quantify the contribution of the Stark effect to the observed broadening. Meanwhile, we cannot rule out the possibility of the broadening due to the Stark effect because of the high electron density in the plasma plume as shown above. However, at the same time, we know that the atomic density of the plume is very high, which may exceed 10^{21} cm^{-3}, as has been suggested by our previous work.[34] Furthermore, the time dependence of the linewidth shows a rather slow decrease compared with the decrease of the continuous spectral component of the emission spectra, suggesting a broadening mechanism other than Stark broadening, i.e., the mechanism which is not directly related to the plasma electrons. For atoms and molecules, the collision frequency $Nv\sigma$ is estimated to be 2.9×10^{10} s^{-1} in the early time range, where the molecular number density N is assumed to be 10^{20} cm^{-3}, the average velocity v is estimated from the Maxwell–Boltzmann distribution at 6000 K, and the collision cross section σ is assumed to have 0.2 nm radius. This collision frequency is comparable to the half width at half maximum broadening of the observation at 50 ns (Fig. 5). Although we do not have clear evidence so far, it seems that the collision broadening is the dominant mechanism for the broadening of the C_2 rotational lines.

D. Time evolution of the plume

In the following discussion, we focus our attention mainly on the time evolution of the ablation plume produced at solid–liquid interfaces. When the absorption of incident laser energy exceeds a threshold, the surface of the target is sufficiently excited or heated to eject surface species in the form of atoms, ions, and molecules. Until the delay time of approximately 50 ns, plasma is present in this region, as evidenced by the spectrally continuous radiation as seen in Fig. 2. The Swan band superposed to the continuous spectrum suggests that C_2 molecules are already formed in this time scale, although the rotational lines are not so clear as to enable the temperature determination by the present method. However, by fitting the continuous spectra to the Planck formula of blackbody radiation, the electron temperature could be estimated. The previous study gave several thousand degrees,[15] e.g., $\sim$7400 K at 59 ns in the case of laser ablation of graphite in water. The decrease of the continuous spectra corresponds to the extinction of plasma electrons. After the continuous spectrum vanishes, the emission lines from C_2 molecules are clearly resolved, which enables us to obtain rotational temperature quantitatively.

The ablated species were confined in a small region due to the presence of a liquid, as has been evidenced previously by the imaging of the light emitting region.[34] The water-confined structure causes a high density and high pressure of the ablated species, and therefore, the collision frequency is extremely large, compared with that in vacuum. Actually, the pressure at around 20 ns of the delay time was estimated to be sub-GPa from the size of the plume and the amount of the ablated species.[34] The linewidth in Fig. 5 suggests that the collision frequency of C_2 molecules keeps the same order of magnitude for more than 1000 ns. At the same time, the light emitting region is gas-cavity-like in this time range as evidenced by the rotation of C_2 molecules.

In order to clarify the behavior of the ablated species after the extinction of the light emission, we need to detect dark species or the ground state species. In our preliminary results of shadow-graph measurements, it was observed that the plume region expands, reaches the maximum size at ~100 μs of the delay time, and collapses at ~250 μs. The size of the shadow image extrapolated to 0.1 μs coincides with the observed size[34] of the light emitting region at this delay time. The time scale of the cavity expansion is so slow compared with the extinction of the light emission that the cavity size in the time range of the emission measurement is virtually unchanged. This is consistent with the emission image measurements, which show a constant size of the emission region from 20 to 100 ns,[34] if we assume that the whole cavity region emits light.

The intensity of the Swan band becomes lower than the detection limit at a delay time of $\sim$2000 ns. This is a direct consequence of further temperature decrease in this region as well as the decreasing population of C_2 molecules due to the coagulation of carbon species to form clusters. As shown in Fig. 4, the temperature in this region starts to decrease at around 1000 ns. Although the present results give data only up to 1200 ns, the temperature of the plume decreases obviously toward equilibrium with the surrounding liquid. Also, the pressure decrease should accompany the temperature decrease. Nanosized clusters in their high-pressure phases of the ablated material, as observed in the literature,[20] are most probably produced in this time range. If the clusters grow in this experimental setup, the size would be limited to the order of nanosize because of this strictly limited time to grow. However, it should be noted that further evidence is required to complete this discussion.

VI. CONCLUSION

We studied in detail the rotational temperature of C_2 molecules in the laser ablation plume produced by the irradiation of a graphite target in water. The temperature was obtained as a function of time, and was compared with those obtained in air atmosphere.

Emission spectra of the (0,0) Swan band of C_2 molecules were observed. The observation of clearly resolved rotational lines suggests that the C_2 molecules are rotating and that the

interaction of C_2 molecules with surrounding species is not as strong as the case of being dissolved in liquid, which means that the ablated species form a gas-cavity-like region.

Rotational temperature and linewidth were obtained as adjusting parameters in the fitting process using a band-tail region of the (0,0) Swan band. The resultant temperature of the plume produced at the water–graphite interface was ~6000 K and started to decrease at ~1000 ns of the delay time, in contrast to the plume in air showing a rather gradual decrease of the temperature. The linewidth obtained as a best-fit parameter suggests collision broadening as a result of the high density of energetic species confined in a small region due to the presence of water. The ablated species in liquid form a high-density, high-pressure, and high-temperature region.

ACKNOWLEDGMENTS

The authors gratefully acknowledge Kokichi Hotta for his technical support. This work was financially supported by the Grant-in-Aid for Scientific research from the Japan Society for the Promotion of Science.

[1] R. Casaes, R. Provencal, P. Joshua, and R. J. Saykally, J. Chem. Phys. **116**, 6640 (2002).
[2] S. A. Beaton and M. C. L. Gerry, J. Chem. Phys. **110**, 10715 (1999).
[3] Z. Mingfei, G. V. Chertihin, and L. Andrews, J. Chem. Phys. **109**, 10893 (1998).
[4] S. M. Park and J. Y. Moon, J. Chem. Phys. **109**, 8124 (1998).
[5] M. Yoshimoto, K. Yoshida, H. Maruta, Y. Hishitani, H. Koinuma, S. Nishio, M. Kakihana, and T. Tachibana, Nature (London) **399**, 340 (1999).
[6] N. Chunming, Y. Z. Lu, and C. M. Lieber, Science **261**, 334 (1993).
[7] T. Kawai, Y. Egami, H. Tabata, and S. Kawai, Nature (London) **349**, 200 (1991).
[8] R. S. Lee, H. J. Kim, J. E. Fischer, A. Thess, and R. E. Smalley, Nature (London) **388**, 255 (1997).
[9] Y. Zhang, K. Suenaga, C. Colliex, and S. Iijima, Science **281**, 973 (1998).
[10] D. Bäuerle, *Laser Processing and Chemistry* (Springer, Berlin, 2000).
[11] J. C. Miller, in *Laser Ablation: Principles and Applications*, edited by J. C. Miller (Springer, Berlin, 1994).
[12] P. P. Patil, D. M. Phase, S. A. Kulkarni, S. V. Ghaisas, S. K. Kulkarni, S. M. Kanetkar, S. B. Ogale, and V. G. Bhide, Phys. Rev. Lett. **58**, 238 (1987).
[13] S. B. Ogale, P. P. Patil, D. M. Phase, Y. V. Bhandarker, S. K. Kulkarni, S. A. Kulkarni, V. G. Bhide, and S. Guha, Phys. Rev. B **36**, 8237 (1987).
[14] A. Wakisaka, J. J. Gaumet, Y. Shimizu, Y. Tamori, H. Sato, and K. Tokumaru, J. Chem. Soc., Faraday Trans. **89**, 1001 (1993).
[15] T. Sakka, S. Iwanaga, Y. H. Ogata, A. Matsunawa, and T. Takemoto, J. Chem. Phys. **112**, 8645 (2000).
[16] A. Dupont, P. Caminat, P. Bournot, and J. P. Gauchon, J. Appl. Phys. **78**, 2022 (1995).
[17] V. A. Ageev, A. Fbokhonov, V. V. Zhukovskii, and A. A. Yankovskii, J. Appl. Spectrosc. **64**, 683 (1997).
[18] L. Berthe, R. Fabbro, P. Peyre, L. Tollier, and E. Bartnicki, J. Appl. Phys. **82**, 2826 (1997).
[19] S. Zhu, Y. F. Lu, M. H. Hong, and X. Y. Chen, J. Appl. Phys. **89**, 2400 (2001).
[20] J. B. Wang and G. W. Yang, J. Phys.: Condens. Matter **11**, 7089 (1999).
[21] Y. F. Lu, S. M. Huang, X. B. Wang, and Z. X. Shen, Appl. Phys. A: Mater. Sci. Process. **A66**, 543 (1998).
[22] J. Singh, M. Vellaikai, and J. Narayan, J. Appl. Phys. **73**, 4351 (1993).
[23] H. R. Griem, *Principles of Plasma Specroscopy* (Cambridge University Press, Cambridge, U.K., 1997).
[24] G. Herzberg, *Molecular Spectra and Molecular Structure* (Krieger, Malabar, FL, 1950), Vol. 1.
[25] S. Pellerin, K. Musiol, O. Motret, B. Pokrzywka, and J. Chapelle, J. Phys. D **29**, 2850 (1996).
[26] Y. Yamagata, A. Sharma, J. Narayan, R. M. Mayo, and J. W. Newman, J. Appl. Phys. **86**, 4154 (1999).
[27] X. Duten, A. Rousseau, A. Gicquel, and P. Leprince, J. Appl. Phys. **86**, 5299 (1999).
[28] E. B. Flint and K. S. Suslick, Science **253**, 1397 (1991).
[29] P. Rousselot, G. Moreels, J. Clairemidi, B. Goidet-Devel, and H. Boehnhardt, Icarus **114**, 341 (1995).
[30] P. Rousselot, J. Clairemidi, and G. Moreels, Astron. Astrophys. **286**, 645 (1994).
[31] T. Sakka, K. Saito, and Y. H. Ogata, Appl. Surf. Sci. **197**, 246 (2002).
[32] I. Kovacs, *Rotational Structure in the Spectra of Diatomic Molecules* (Akadémiai Kiadó, Budapest, 1969).
[33] I. Kovacs, Astrophys. J. **145**, 634 (1966).
[34] K. Saito, K. Takatani, T. Sakka, and Y. H. Ogata, Appl. Surf. Sci. **197**, 56 (2002).
[35] T. Sakka, K. Takatani, and Y. H. Ogata, J. Phys. D **35**, 65 (2002).
[36] H. S. Carslaw and J. C. Jaeger, *Conduction of Heat in Solid* (Oxford University Press, London, U.K., 1946).